Chapter 5
Matrix Choice

Yuki Sugiura, Mitsutoshi Setou, and Daisuke Horigome

Abstract In this section, the choices of matrix compound and solvent composition appropriate for tissue IMS are reviewed. As is well known, it is very important to choose an appropriate matrix for successful imaging measurement. A practical choice of matrix depends upon the type of analyte involved. Until today, in traditional MALDI-MS, a large variety of compounds has been empirically tested for their suitability in playing the role of a matrix; today, researchers can choose from a relatively small number of established "organic chemical matrices" such as sinapic acid (SA), α-cyano-4-hydroxy-cinnamic acid (CHCA), and 2,5-dihydroxybenzoic acid (DHB), and they have proven to be useful matrices for MALDI-imaging measurement. On the other hand, in MALDI-IMS, it is still necessary to develop a new matrix because of the extremely complex chemistry on the tissue surface. We also introduce some novel organic matrices and the further use of nanoparticles as an alternative to organic matrices from recent literature.

5.1 Principle of Molecular Ionization

Two ionization methods – matrix-assisted laser desorption/ionization (MALDI) and secondary ion mass spectrometry (SIMS) – are widely used for performing IMS with tissue sections [1]. MALDI-MS can measure large mass ranges of ions in a tissue section, and it can also perform molecular identification via tandem mass

Y. Sugiura
Department of Bioscience and Biotechnology, Tokyo Institute of Technology,
4259 Nagatsuta-cho, Midori-ku, Yokohama, Kanagawa 226-8501, Japan

Y. Sugiura and M. Setou (✉)
Department of Molecular Anatomy, Hamamatsu University School of Medicine,
1-20-1 Handayama, Higashi-ku, Hamamatsu, Shizuoka 431-3192, Japan
e-mail: setou@hama-med.ac.jp

D. Horigome
Mitsubishi Kagaku Institute of Life Sciences, 11 Minamiooya, Machida, Tokyo, Japan

spectrometry (MS^n). If compared, SIMS can ionize the $m/z < 1000$ range of ions; at that point, it can hardly perform molecular identification by tandem mass spectrometry. On the other hand, SIMS-based IMS has a much higher spatial resolution (a few hundred nanometers) than that of MALDI-IMS (dozens of micrometers), as a result of the tightly focused primary ion beam that is narrower than the UV-pulsed laser beams of MALDI (see details of SIMS in Part VIII).

MALDI is a soft ionization technique allowing the analysis of large biomolecules (biopolymers such as proteins, peptides, and sugars) and large organic molecules (such as polymers, dendrimers, and other macromolecules) [2]. It is carried out by co-crystallizing the analyte and matrix and ionization triggered by irradiating laser to the co-crystal. The matrix compound is excited by absorbing laser energy, which is converted into heat; the heat then evaporates part of the analyte molecules [3]. The matrix is then thought to transfer part of its charge to the analyte molecules, thus ionizing them while still protecting them from the disruptive energy of the laser.

Protonated and deprotonated molecules are generally designated as $[M+H]^+$ and $[M-H]^-$, respectively. If alkali metal ions such as sodium and potassium are contained in the co-crystal (as is often true for biological tissue samples), sodium adduct $[M+Na]^+$ and potassium adduct $[M+K]^+$ ions are also generated. Such a soft ionization technique was first reported by Tanaka et al. (1988), who enhanced the subsequent development of MS for biomolecules and large organic molecules [4]. Subsequent studies have excellently improved the soft ionization method, which had previously limited the molecular weight of the analyte to the extent of 10 kDa for peptides/proteins; those studies have developed the chemical matrices used today, which push the measurable mass range to around 100 kDa [2].

5.2   Choice of Matrices

The essential functions required for the matrix in measuring biological macromolecules in MS are as follows:

1. Isolate analyte molecules by dilution and prevent analyte aggregation
2. Stabilize the matrix–analyte co-crystal in the vacuum chamber
3. Absorb laser energy via electronic excitation
4. Disintegrate the condensed phase of the co-crystal without excessive destructive heating of the embedded analyte molecules

It is very important to choose an appropriate matrix for successful imaging. A practical choice depends upon the type of analyte involved. Up to now, for traditional MALDI-MS, a large variety of compounds has been empirically tested for their suitability in playing the role of a matrix; today, researchers can choose from a relatively small number of established "organic chemical matrices," e.g., benzoic or cinnamic acid derivatives, and these are also available for MALDI imaging measurement. For example, sinapic acid is commonly used for imaging of relatively
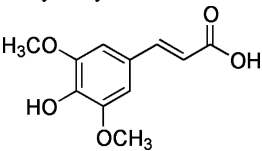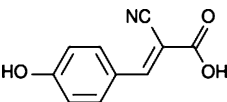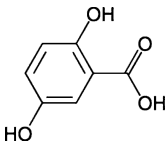
high molecular weight proteins, whereas 2,5-dihydroxybenzoic acid (DHB) is applied to small organic compounds, such as lipids. The properties of the three major matrices used for the MALDI-MS analysis of tissue sections are summarized in Table 5.1.

On the other hand, in MALDI-IMS, it is constantly necessary to search for potential matrix compounds because of the extremely complex chemistry on the tissue surface. Improvements to the current chemical matrices in terms of mass resolution, ionization efficiency, and measurable molecular weight range are essential for development of IMS methodology, because direct tissue analyses generally lead to a lowered spectral quality – likely the result of the nature of the complex chemistry in direct tissue MALDI-MS, involving numerous factors (e.g., thickness, freezing date, or type of tissue). Below, we introduce some of these challenges.

5.2.1 Ionic Matrices

Ionic matrices comprising organic acids and organic bases, in particular, have attracted attention over the years [5]. By applying simple synthetic processes vis-à-vis acid–base reactions, solid ionic matrices can be produced. For example, by

Table 5.1 Three major matrices used with MALDI-MS

| Matrix	SA	CHCA	DHB
Other name	• Sinapinic acid • 3,5-Dimethoxy-4-hydroxycinnamic acid	• α-Cyano-4-hydroxycinnamic acid	• 2,5-Dihydroxy benzoic acid
Structural formula			
MW	224.21	189.17	154.12
Chemical formula	$C_{11}H_{12}O_5$	$C_{10}H_7NO_3$	$C_7H_6O_4$
Solubility	• Low solubility in H_2O • Soluble in methanol/ H_2O and polar organic solvents	• Low solubility in H_2O • Soluble in methanol/ H_2O and polar organic solvents	• Soluble in H_2O • Soluble in methanol/H_2O and polar organic solvents
Feature	High signal-to-noise ratio		The quality of a mass spectrum largely depends on the quality of the matrix's crystal
Subject	Protein (4–30 kDa)	Lipid and peptides (~8 kDa)	Lipid and peptides (~5 kDa)
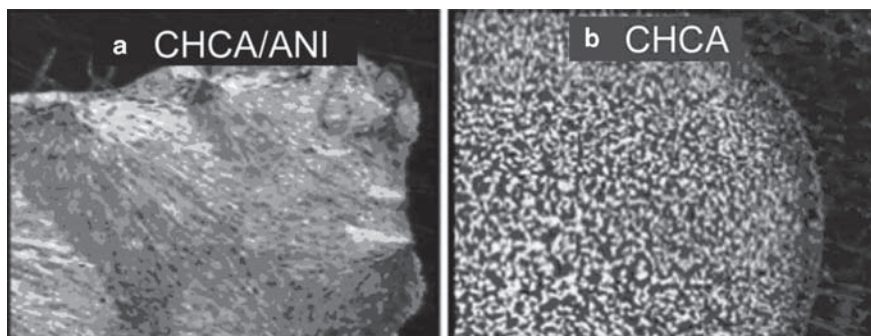
Fig. 5.1 Photographs of the matrix crystals of CHCA/ANI (**a**) in comparison with conventional CHCA (**b**). (Reprinted from Lemaire et al., Anal Chem 78(3):809–819.)

adding an equimolar amount of aniline (ANI) to the conventional matrix compound CHCA in methanol and subsequently evaporating the solvent, one can produce powdered CHCA/ANI. The solid ionic matrix is dissolved in the solvent [2:1 acetonitrile/0.01% trifluoroacetic acid (TFA)] at a concentration of 10 mg ml^{-1}. This ionic matrix can form extremely dense matrix crystals on a tissue section (Fig. 5.1) [6]. Compared to the conventional CHCA matrix, the CHCA/ANI matrix can achieve a much higher quality of IMS consequent to its better signal-to-noise (S/N) ratio (Fig. 5.2) [6]. Spectrum improvements attributed by the CHCA/ANI matrix resulted in better ion image quality than when using a conventional matrix (Fig. 5.3), in terms of increased signal detection and improved dynamic range of ion intensity, with reproducibility [6].

5.2.2 Challenges for Imaging of Primary Metabolites in m/z < 1,000 Region

Regarding imaging of low molecular weight compounds, one of the disadvantages of organic matrices is the number of mass peaks in the low m/z range. The low m/z region (<m/z 1,000) of a MALDI spectrum contains a large population of ions from endogenous metabolites as well as matrix-related adduct clusters and fragments, which are clearly seen in the MALDI ion mobility spectrum obtained on the tissue section (Fig. 5.4) [7, 8]. Such high density of ions increases the risk for sharing the same mass window by matrix ions and analyte molecules.

Recently, 9-aminoacridine (9-AA) was reported to exhibit very few matrix interferences in the low-mass range (m/z < 500) [10] and thus enables us to image primary metabolites in a MALDI imaging experiment [11, 12]. Benabdellah et al. reported that with appropriate sample preparation protocol, 9-AA exhibits almost no matrix interference, and they successfully detected and identified 13 primary metabolites (AMP, ADP, ATP, UDP-GlcNAc, etc.) on the rat brain section, in negative ion detection mode
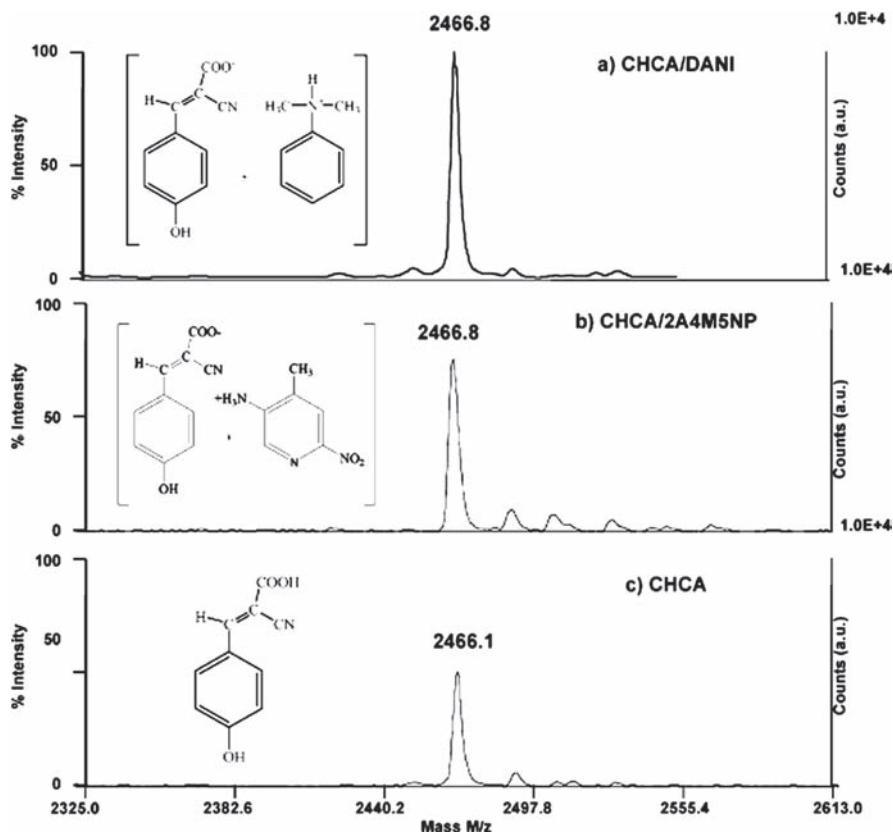
Fig. 5.2 Typical MALDI mass spectrum obtained for ACTH 18-39 (1 pmol) in the linear negative ion mode using CHCA/DANI (**a**), CHCA/2A4M5NP (**b**), and CHCA (**c**) as matrix. Ionic matrix formula is enclosed to each mass spectrum. (Reprinted from Lemaire et al., Anal Chem 78(3): 809–819.)

(Fig. 5.5) [12]. In addition, Burrell et al. also demonstrated that, by use of the 9-AA in positive ion detection mode, localization of sugar and phosphorylated metabolites such as glucose-6-phosphate can be clearly imaged in plant tissues (Fig. 5.6) [11].

These advances are quite important to develop MALDI-IMS as a practical tool for metabolite imaging in the clinical and biological field, because, until today, we did not have established imaging technique for such primary metabolites.

5.2.3 Nanoparticle-Based IMS

One of the critical limitations of the spatial resolution of MALDI-IMS is the size of the organic matrix crystal and the analyte migration during the matrix application process. To overcome these problems, our research group reported a nanoparticle-assisted
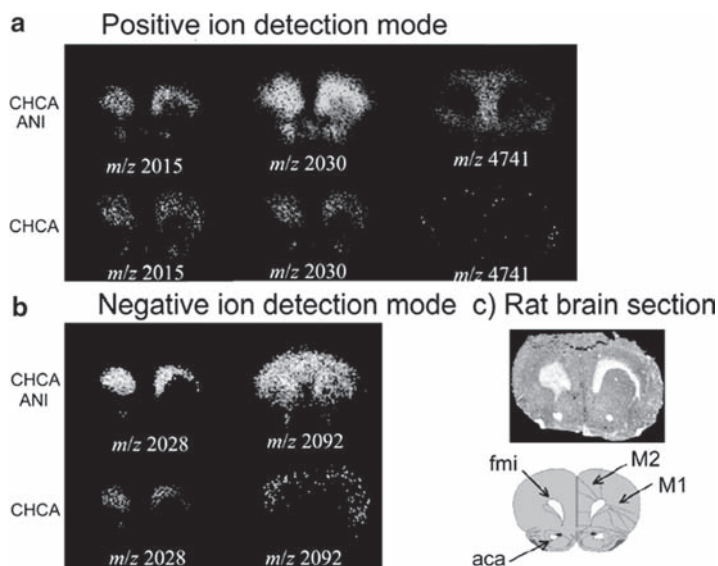
Fig. 5.3 MALDI-IMS using MALDI LIFT-TOF in reflector mode at 50-Hz repetition rate with ionic matrixes CHCA/ANI and CHCA in positive (**a**) and negative modes (**b**). MALDI imaging can be compared with rat brain anatomy. For CHCA/ANI and CHCA, acquisitions in both polarities were performed on the same rat brain cut (**c**) Optical image and corresponding atlas of rat brain section. (Reprinted from Lemaire et al., Anal Chem 78(3):809–819.)
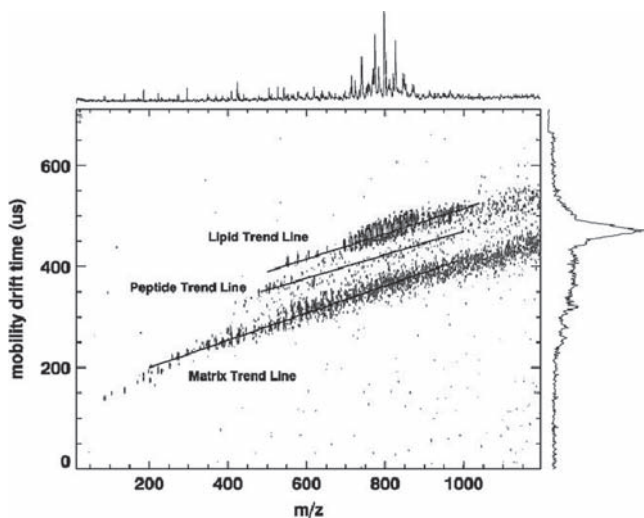

Fig. 5.4 MALDI ion mobility two-dimensional (2D) plot of a rat brain tissue section with DHB matrix in positive ion detection mode. Many of the peaks in the trend line identified as "matrix" can be assigned to DHB clusters or DHB clusters + potassium. (See details of MALDI ion-mobility MS in Chap. 17). (Reprinted from Jackson et al., J Mass Spectrom 42:1093–1098.)
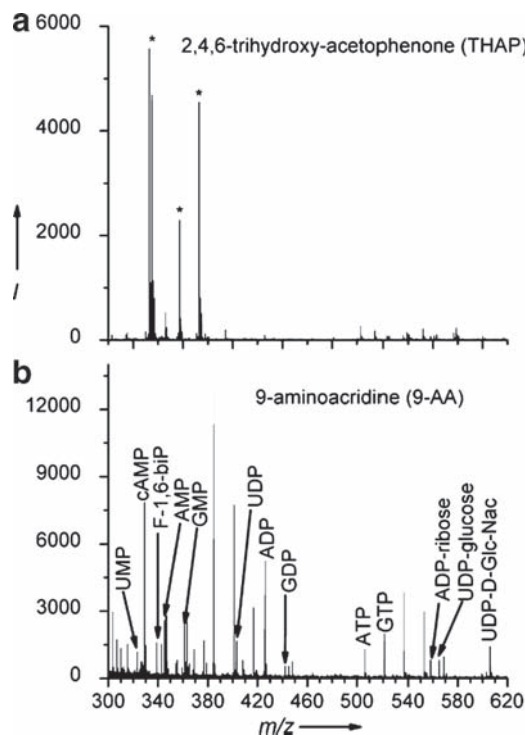
Fig. 5.5 MALDI-MS spectra in the negative ion mode acquired from a rat brain tissue section with matrix solution of (**a**) 2,4,6-trihydroxyacetophenone (THAP) and (**b**) 9-aminoacridine (10 mg ml^{-1}, in methanol) deposited on the section. *Asterisk*, matrix peaks. (Reprinted from Benabdellah et al., Anal Chem 81(13):5557–5560.)

laser desorption/ionization (nano-PALDI)-based IMS [13], in which the matrix crystallization process is eliminated [14]. In nano-PALDI, spatial resolution is not restricted by the crystal size but only by the instrumental factor (such as laser spot diameter); thus, the use of functionalized nanoparticle (fNP, $d=\sim3.5$ nm) as matrix has enabled researchers to image compounds with high spatial resolution at the cellular level.

Figure 5.7 shows an overview of nano-PALDI. As already mentioned, SIMS-based IMS is useful for direct biomolecular analysis at high spatial resolution without interference from the matrix background signal; however, the typical SIMS technique has rarely been used for MS^n analysis [15] and is limited to low molecular analysis. In this regard, nano-PALDI enables researchers to ionize relatively heavy molecules even up to the insulin molecule (MW 5,773) (Figs. 5.7 and 5.8) [16]. As another important advantage, spraying fNP on the tissue surface did not alter the optical image of the tissue structure (Fig. 5.8g,h). Furthermore, its ability to eliminate the matrix-derived signals is important, for analysis of small molecules [14, 17].
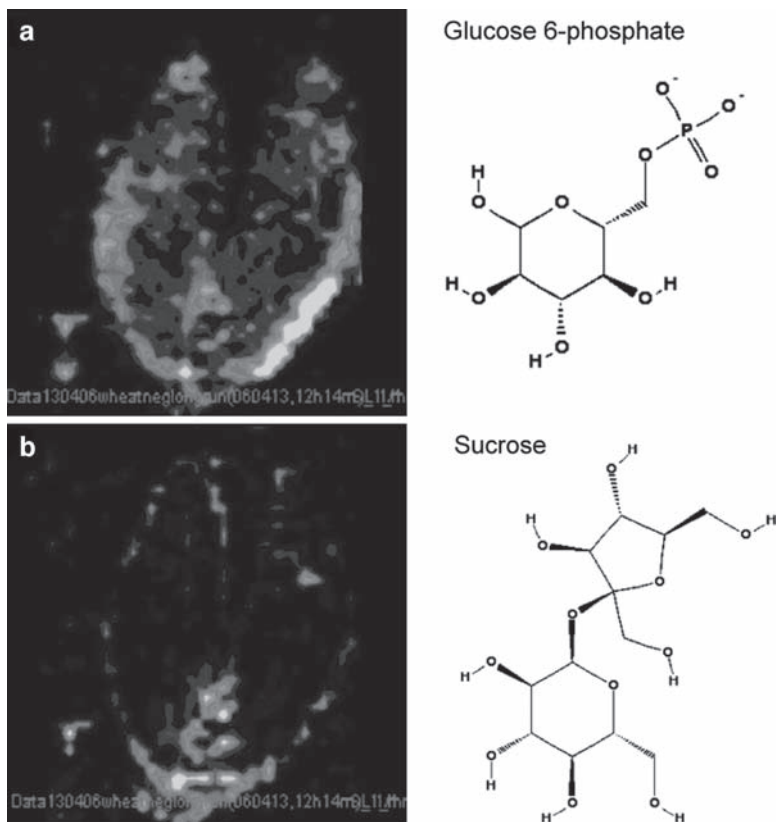
Fig. 5.6 IMS of glucose-6-phosphate and sucrose in developing wheat seeds: MALDI-IMS results for glucose 6-phosphate (**a**) and sucrose in wheat plant section (**b**). Intensity is plotted from *black* to *white* with white being the greatest signal. 9-AA (10 mg ml^{-1}, in acetone containing 0.1% TFA) was used as matrix. (Reprinted from Burrell et al., J Exp Bot 58:757–763.)

Because of their attractive features, nanoparticles are increasingly used as ionization-enhancing reagents as an alternative to organic matrices in IMS. Recently, gold nanoparticles ($d = \sim 5.5$ nm) have been used in MS [18] and IMS [9]. Gold NPs ionize biomolecules that are difficult to detect using traditional organic matrices because of the unique ionization process [9].

5.3 Composition of Matrix Solvent

Composition of the matrix solvent and further matrix/solvent combination is also an important issue to optimize for successful imaging of the researcher's interest analyte. The goal of optimization the matrix solution is to effectively extract the
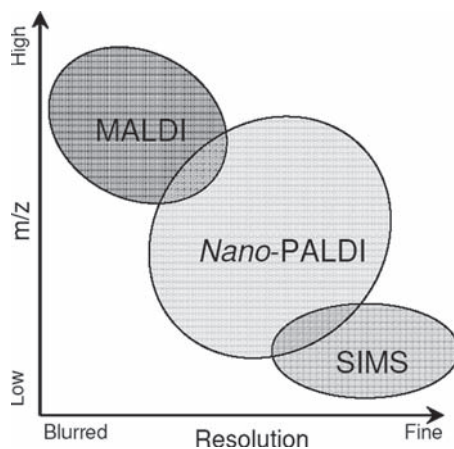
Fig. 5.7 Overview of nanoparticle-assisted laser desorption/ionization (nano-PALDI). Nano-PALDI can achieve high spatial resolution as in SIMS, and analysis of high molecules as in MALDI-IMS reprinted from [14]

analyte of interest while suppressing extraction of other molecular species from the tissues. Thus, optimal solvent composition will vary depending on the molecule to be analyzed as well as the type of tissue sample being analyzed [19].

Figure 5.9 demonstrates that organic solvent concentration in the matrix solution affects the detection of lipids and peptides. The results indicate that lipids and peptides could be efficiently extracted from tissue sections into organic and nonorganic solvents, respectively. Thus, for imaging of small molecules including peptides without a tissue-washing process (see Chap. 4), the results showed that a high composition of methanol was favorable for lipid detection whereas a low concentration solution was favorable for the detection of endogenous peptides. We additionally note that composition of the solvent also affects matrix–analyte co-crystal form; using DHB, needle-like (from which peptides were detected) changed into aggregates of smaller crystals (from which lipids were detected) (Fig. 5.9b). Because generation of a minute and homogeneous crystal layer among the tissue surface is required, when optimizing the matrix solvent, researchers should be aware of this issue as well as sensitivity of signal detection.

For protein analysis, one cannot also categorically describe which solvent is the best because the result of a solvent varies according to the type of tissue involved. For example, Shwartz et al. tested a series of saturated SA solutions in varying organic solvent/water combinations on a mouse liver section, and reported that an ethanol mixture is the best solvent so far for use with a mouse liver section whereas an acetonitrile mixture is the best one so far for use with a rat brain section [19]. Further, even for the same organ tissue sections, certain signal peaks have been observed only with an ethanol mixture solvent, whereas certain other signal peaks have been detected only when an acetonitrile mixture solvent was used (Fig. 5.10) [19]. Interestingly, those signal peaks could not be measured by using a three-in-one admixture (25:25:50 ethanol/acetonitrile/0.1% TFA in water).
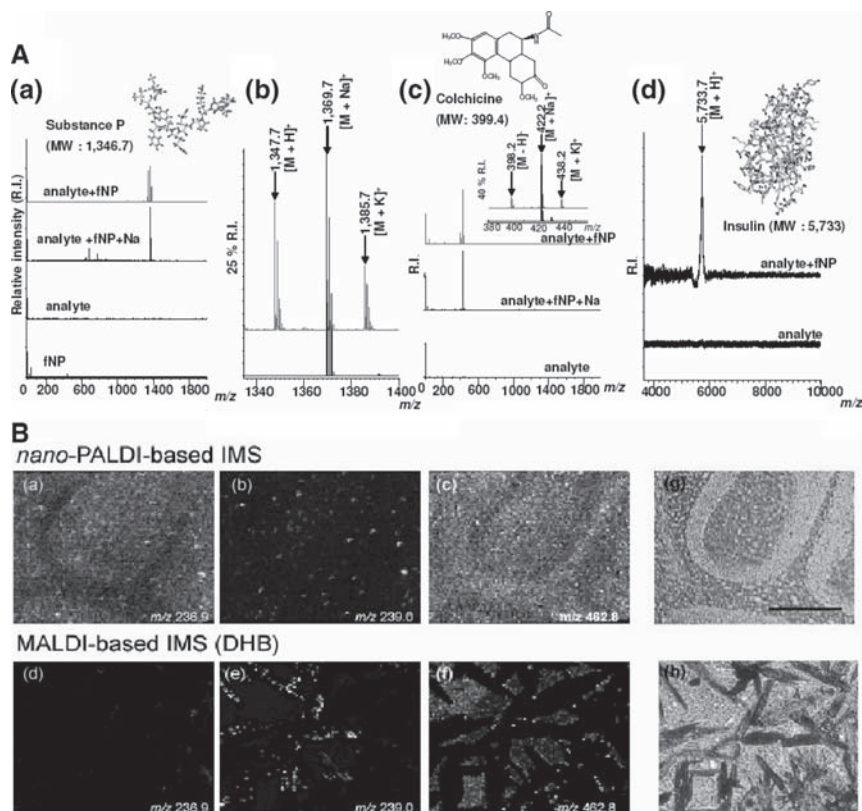
Fig. 5.8 Nano-PALDI MS and IMS. **A** The authors evaluated the usefulness of functional nanoparticles (NP) (fNP) in assisting ionization by using various analyte molecules. For peptide, in a spectra measured in an absence of external sodium acetate, signals for a proton, a sodium adduct, and a potassium adduct of substance P (MW 1,346.7) were observed. In the case of the colchicine drug (MW 399.4) (**c**) and insulin (MW 5,733) (**d**), fNP also facilitated ionization of the analytes, indicating that these can function as ionization-assisting reagents over a wide range of analytes. **B** Ion images obtained with the fNP (**a–c**) and with DHB (**d–f**) matrix. nano-PALDI can clearly provide each ion distribution images (**a–c**). However, from the DHB-sprayed section, several ions showed no significant distribution image (**e**), and were detected only from needle crystals (**e**) or the noncrystal region (**f**). Optical images of rat cerebellum tissues coated with the fNP (**g**) and with DHB (**h**) are also shown. *Bar* 500 μm (Reprinted from Taira et al., Anal Chem 80(12):4761–4766.)

As different solvent composition affects the overall protein profile, changing the concentration of TFA also changes the specific molecules measured. It has also been reported that a high concentration (>2%) of TFA can degrade a few signal peaks that could otherwise be detected with a solvent composition with a lower concentration of TFA [19], indicating that a high concentration of TFA is not recommended.

Overall, for protein analysis, a mixture of equal polar organic solvent (50% acetonitrile or ethanol) and 0.1–0.5% TFA in water is commonly used as the first choice of solvent and is recommended to be modified to obtain optimal performance.
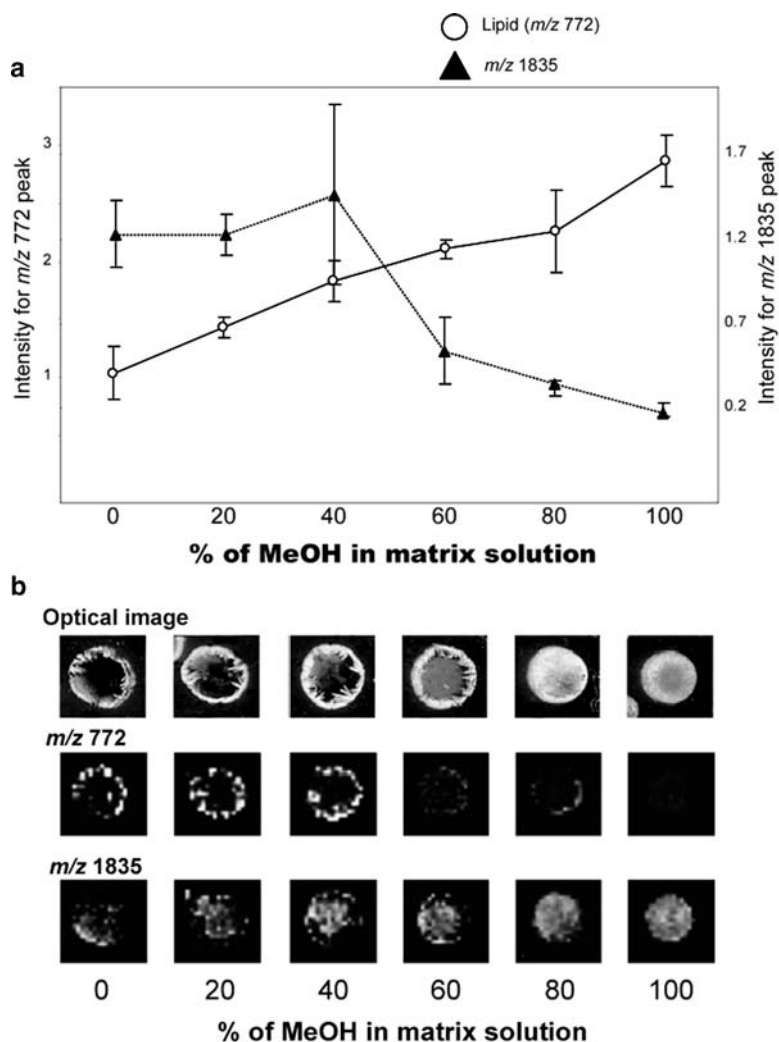
Fig. 5.9 Organic solvent concentration in the matrix solution affects the detection of lipids and peptides. **a** Matrix solutions with different water/methanol ratios (0%, 20%, 40%, 60%, 80%, and 100% methanol containing 0.1% TFA) were prepared. Then, 0.5 µl of each solution was spotted onto the brain homogenate sections ($n=3$). **b** Optical and ion images of the m/z 772 (lipid) and m/z 1,835, presumably derived from a peptide molecule. At high methanol concentrations, peptide detection was suppressed and lipid detection was favored (Reprinted from Sugiura et al., Rapid Commun Mass Spectrom 23:3269–3278.)

Finally, Table 5.2 summarizes the representative examples of matrix–solvent combination for IMS of various molecular species. Exploring the optimal matrix–solvent combination for each researcher's experiment, based on previous studies introduced here, is the key for successful IMS.
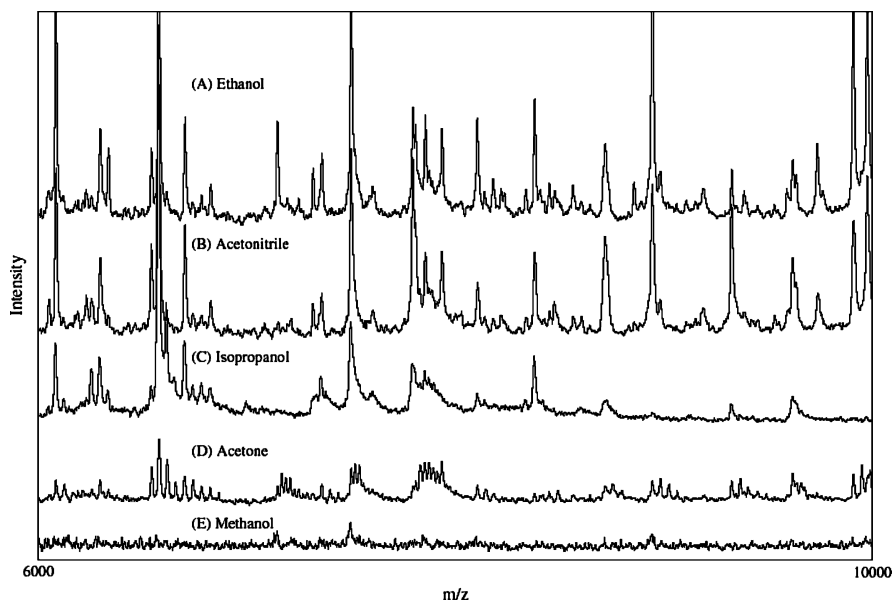
Fig. 5.10 Solvent composition affects the tissue protein profile. Saturated sinapinic acid matrix in solvents of 50:50 organic solvent/0.1% TFA in water as shown was deposited onto mouse liver tissue sections. The use of different solvent systems results in different protein profiles. Overall 50:50 ethanol/0.1% TFA resulted in the best protein profile for the mouse liver section, but 50:50 acetonitrile/0.1% TFA in water has been shown to give better profiles for other organs (such as rat brain). (Reprinted from Schwartz et al., J Mass Spectrom 38:699–708.)

Table 5.2 Representative examples of matrix/solvent combination for IMS of various molecular species

Analyte	Polarity	Matrix compound	Concentration (mg ml^{-1})	Solvent	Additives	Reference
Protein/peptide	POS	SA	Saturated	50% Acetonitrile, 0.1% TFA, 50% ethanol 0.1% TFA	–	Schwartz et al. 2003 [19]
Protein/peptide	POS	SA	25	50% Acetonitrile, 0.1% TFA	–	Seeley et al. 2008 [20]
Protein/peptide	POS	CHCA	10	50% Ethanol, 0.1% TFA	–	Altelaar et al. 2007 [21]
Drug	POS	CHCA	10	50% Acetonitrile, 0.1% TFA	–	Hopfgartner et al. 2009 [22]
Drug	POS	CHCA	25	Ethanol, 1% TFA	–	Atkinson et al. 2007 [23]
Phospholipids	POS	DHB	40	70% MeOH	Sodium acetate	Garrett et al. 2006 [7]
Phospholipids	POS/NEG	DHB	50	70% MeOH	Potassium acetate	Sugiura et al. 2009 [24]
Phospholipids	POS/NEG	MBT[a]	Saturated	MeOH	Cesium chloride	Astigarraga et al. 2008 [25]
Phospholipid (cardiolipin)	NEG	DHA[b]	30	50% Ethanol	Cesium iodide	Wang et al. 2007 [26]
Sugar/phosphorylated metabolites	POS	9-AA	10	Acetone, 0.1% TFA	–	Burrell et al. 2007 [11]
nucleotides	NEG	9-AA	10	MeOH	–	Benabdellah et al. 2009 [12]

POS positive ion detection mode, *NEG* negative ion detection mode

[a]MBT, 2-mercaptobenzothiazole

[b]DHA, 2,6-dihydroxyacetophenone

References

1. McDonnell LA, Heeren RM (2007) Imaging mass spectrometry. Mass Spectrom Rev 26:606–643
2. Karas M, Bachmann D, Bahr U, et al. (1987) Matrix assisted ultraviolet-laser desorption of non-volatile compounds. Int J Mass Spectrom Ion Processes 78:53–68
3. Dreisewerd K (2003) The desorption process in MALDI. Chem Rev 103:395–426
4. Tanaka K, Waki H, Ido Y, et al. (1988) Protein and polymer analyses up to m/z 100,000 by laser ionization time-of flight mass spectrometry. Rapid Commun Mass Spectrom 2:151–153
5. Armstrong DW, Zhang LK, He L, et al. (2001) Ionic liquids as matrixes for matrix-assisted laser desorption/ionization mass spectrometry. Anal Chem 73:3679–3686
6. Lemaire R, Tabet JC, Ducoroy P, et al. (2006) Solid ionic matrixes for direct tissue analysis and MALDI imaging. Anal Chem 78:809–819
7. Garrett TJ, Prieto-Conaway MC, Kovtoun V, et al. (2006) Imaging of small molecules in tissue sections with a new intermediate-pressure MALDI linear ion trap mass spectrometer. Int J Mass Spectrom 260:11
8. Cornett DS, Frappier SL, Caprioli RM (2008) MALDI-FTICR imaging mass spectrometry of drugs and metabolites in tissue. Anal Chem 80:5648–5653
9. Jackson SN, Ugarov M, Egan T, et al. (2007) MALDI-ion mobility-TOFMS imaging of lipids in rat brain tissue. J Mass Spectrom 42:1093–1098
10. Amantonico A, Oh JY, Sobek J, et al. (2008) Mass spectrometric method for analyzing metabolites in yeast with single cell sensitivity. Angew Chem (Int Ed) 47:5382–5385
11. Burrell M, Earnshaw C, Clench M (2007) Imaging matrix assisted laser desorption ionization mass spectrometry: a technique to map plant metabolites within tissues at high spatial resolution. J Exp Bot 58:757–763
12. Benabdellah F, Touboul D, Brunelle A, et al. (2009) In situ primary metabolites localization on a rat brain section by chemical mass spectrometry imaging. Anal Chem 81, 5557–5560
13. Moritake S, Taira S, Sugiura Y, et al. (2009) Magnetic nanoparticle-based mass spectrometry for the detection of biomolecules in cultured cells. J Nanosci Nanotechnol 9:169–176
14. Taira S, Sugiura Y, Moritake S, et al. (2008) Nanoparticle-assisted laser desorption/ionization based mass imaging with cellular resolution. Anal Chem 80:4761–4766
15. McMahon JM, Short RT, McCandlish CA, et al. (1996) Identification and mapping of phosphocholine in animal tissue by static secondary ion mass spectrometry and tandem mass spectrometry. Rapid Commun Mass Spectrom 10:335–340
16. Moritake S, Taira S, Sugiura Y, et al. (2008) Magnetic nanoparticle-based mass spectrometry for the detection of biomolecules in cultured cells. J Nanosci Nanotechnol. 2009 (1):169–76.
17. Ageta H, Asai S, Sugiura Y, et al. (2008) Layer-specific sulfatide localization in rat hippocampus middle molecular layer is revealed by nanoparticle-assisted laser desorption/ionization imaging mass spectrometry. Med Mol Morphol 42:16–23 (2009)
18. McLean JA, Stumpo KA, Russell DH (2005) Size-selected (2–10 nm) gold nanoparticles for matrix assisted laser desorption ionization of peptides. J Am Chem Soc 127:5304–5305
19. Schwartz SA, Reyzer ML, Caprioli RM (2003) Direct tissue analysis using matrix-assisted laser desorption/ionization mass spectrometry: practical aspects of sample preparation. J Mass Spectrom 38:699–708
20. Seeley EH, Oppenheimer SR, Mi D, et al. (2008) Enhancement of protein sensitivity for MALDI imaging mass spectrometry after chemical treatment of tissue sections. J Am Soc Mass Spectrom 19:1069–1077
21. Altelaar AFM, Taban IM, McDonnell LA, et al. (2007) High-resolution MALDI imaging mass spectrometry allows localization of peptide distributions at cellular length scales in pituitary tissue sections. Int J Mass Spectrom 260:9
22. Hopfgartner G, Varesio E, Stoeckli M (2009) Matrix-assisted laser desorption/ionization mass spectrometric imaging of complete rat sections using a triple quadrupole linear ion trap. Rapid Commun Mass Spectrom 23:733–736

23. Atkinson SJ, Loadman PM, Sutton C, et al. (2007) Examination of the distribution of the bioreductive drug AQ4N and its active metabolite AQ4 in solid tumours by imaging matrix-assisted laser desorption/ionisation mass spectrometry. Rapid Commun Mass Spectrom 21:1271–1276
24. Sugiura Y, Konishi Y, Zaima N, et al. (2009) Visualization of the cell-selective distribution of PUFA-containing phosphatidylcholines in mouse brain by imaging mass spectrometry. J Lipid Res J Lipid Res 50: 1776–1788
25. Astigarraga E, Barreda-Gomez G, Lombardero L, et al. (2008) Profiling and imaging of lipids on brain and liver tissue by matrix-assisted laser desorption/ ionization mass spectrometry using 2-mercaptobenzothiazole as a matrix. Anal Chem 80:9105–9114
26. Wang HY, Jackson SN, Woods AS (2007) Direct MALDI-MS analysis of cardiolipin from rat organs sections. J Am Soc Mass Spectrom 18:567–577
27. Suguira Y, Setou M (2009) Selective imaging of positively charged polar and nonpolar lipids by optimizing matrix solution composition. Rapid Commun Mass Spectrom 23(20): 3269–3278